Hydrolytic stability in hemilabile metal–organic frameworks

Lauren N. McHugh,[1] Matthew J. McPherson,[1] Laura J. McCormick,[1,2] Samuel A. Morris,[1] Paul S. Wheatley,[1] Simon J. Teat,[2] David McKay,[1] Daniel M. Dawson,[1] Charlotte E. F. Sansome,[1] Sharon E. Ashbrook,[1] Corinne A. Stone,[3] Martin W. Smith[3] and Russell E. Morris[1,4]

[1]*EaStCHEM School of Chemistry, University of St Andrews, Purdie Building, St Andrews KY16 9ST, UK*

[2]*Advanced Light Source, Lawrence Berkeley National Laboratory, Berkeley, California, 94720, USA*

[3]*Defence Science and Technology Laboratory (Dstl), Porton Down, Salisbury, Wiltshire SP4 0JQ, UK*

[4]*Department of Physical and Macromolecular Chemistry, Faculty of Sciences, Charles University in Prague, Hlavova 8, 128 43 Prague 2, Czech Republic*

Highly porous metal–organic frameworks (MOFs), which have undergone exciting developments over the past few decades, show promise for a wide range of applications. However, many studies indicate that they suffer from significant stability issues, especially with respect to their interactions with water, which severely limits their practical potential. Here we demonstrate how the presence of 'sacrificial' bonds in the coordination environment of its metal centres (referred to as hemilability) endows a dehydrated copper-based MOF with good hydrolytic stability. On exposure to water, in contrast to the indiscriminate breaking of coordination bonds that typically results in structure degradation, it is non-structural weak interactions between the MOF's copper paddlewheel clusters that are broken and the framework recovers its as-synthesized, hydrated structure. This MOF retained its structural integrity even after contact with water for one year while HKUST-1, a compositionally similar material that lacks these 'sacrificial' bonds, loses crystallinity in less than a day under the same conditions.

Metal-organic frameworks (MOFs) comprise metal ions or clusters joined by organic ligands (linkers) into 3D materials. Their main characteristics are extremely high porosity and surface areas, [1] which leads to potential applications as storage and delivery materials,[2-4] and their highly unusual flexibility.[5] However, a major drawback

of MOFs is their relatively low stability, especially when challenged with reactive adsorbates such as water.[6] Water stability is a particular problem when the as-synthesised MOFs have been dehydrated (activated). Since all uses of MOFs that rely on their porosity need to be activated to make them porous in the first place, this lack of stability when water is present can be a serious problem that prevents application in many cases. Increasing the stability of MOFs has therefore been a major goal of recent research.[6-8] Much of this work has concentrated on changing the chemical composition of the MOF itself (either the metal or the linker) to increase the strength of the bonding in the material. Examples of success in this area include the use of high oxidation metal ions, such as Zr^{IV} in MOFs such as UiO-66,[7] and changing the linker units to groups such as pyrazolate,[8] both of which increase metal-linker bond strengths. Other methods use post-synthetic modifications, such as hydrophobic coatings or mixed-matrix composites to 'protect' the MOF from the ingress of water.[9-11] These approaches, while successful in increasing stability, change the chemistry of the material. Such chemical modification often leads to a reduction in the functionality of a solid, sometimes fatally compromising its utility.[6] There is, therefore, a significant need to prepare MOFs exhibiting both the optimum chemical composition for a specific purpose and a hydrolytic stability that allows successful practical application

The adsorption of toxic gases from breathable air for personal protection is an excellent example of where the porosity of MOFs lends itself to real world application. For example, for the removal of amine-based toxic species and other gases containing 'soft' donor atoms (e.g. H_2S) copper-based MOFs would be the adsorbent of choice owing to the strong Cu-adsorbate interaction. The extremely well known HKUST-1[12] (also known as Cu-btc, where btc = benzene-1,3,5-tricarboxylate) is one such material whose chemistry is ideal for adsorbing ammonia and related toxic gases.[13,14] However, despite its high capacity and selectivity for these gases and vapours, it has relatively poor stability when in contact with moisture.[15] Given that all toxic gas removal applications from breathable air take place in humid conditions, the low stability of HKUST-1 makes it sub-optimal for such applications.

In this paper, we report a Cu-based MOF, which we name STAM-17-OEt, whose chemical composition and structure are close to that of HKUST-1 but which exhibits better hydrolytic stability through a new mechanism. This in turn leads to improved performance for ammonia removal in humid conditions compared with HKUST-1.

The strategy by which we accomplish this is analogous to that used in automobile 'crumple zones' that are used to protect passengers from serious injury during road traffic accidents. Crumple zones use weak areas in the chassis structure that are designed to channel energy away from areas that would cause catastrophic damage to the passengers. The same design principle can be used to increase the stability of an activated Cu-based MOF in the presence of moisture through the presence of weak, sacrificial bonds in the material.

On dehydration, STAM-17-OEt adopts a structure in which the open site of a copper centre (which has previously been coordinated to a water molecule) is weakly coordinated to an oxygen atom belonging to an adjacent paddlewheel cluster. It is these weak coordination interactions that act as sacrificial bonds: on rehydration, these weak bonds will break so that the framework converts back to its original hydrated form. The energy released by the adsorption of water serves to break these long Cu-O bonds, rather than Cu-O bonds in the paddlewheel clusters that hold the framework together. Without the presence of these additional weak interactions and the conformational flexibility of the framework, the energy from the adsorption process would likely break at least some of the metal-linker framework bonds indiscriminately, leading to eventual collapse of the MOF structure.

The flexibility of many MOFs is one of their important features. However, the most famous examples of flexibility, such as that which occurs in materials like MIL-53,[16] involve no bond breaking or rearrangement. Another type of flexibility in MOFs occurs when the coordination environment of the metal changes.[17] If bonds change in an uncontrolled manner this can lead to collapse of the structure. However, if the bond breaking process can be controlled, ensuring it only happens at certain places

that do not affect the overall connectivity of the material, the integrity of the structure may be maintained even as some bonds are broken. We have named this type of MOF hemilabile by analogy to ligands used in homogeneous catalysis where a similar process occurs.[18] Our hypothesis is that if the material is hemilabile and allows the possibility of the formation of new weak bonds on removal of the coordinated water molecules, then as water is readsorbed into the material energy released by the metal-water adsorption interaction is used to preferentially break the weak bonds in the structure, leaving the structural integrity of the metal-bridging ligand bonds intact. This mechanism endows STAM-17-OEt with good hydrolytic stability — much better than that of HKUST-1, as unambiguously shown by a side-by-side test, despite the two MOFs being so close to each other in terms or both chemical composition and structure.

Results and Discussion

Synthesis and crystallography We have prepared a copper-based MOF, STAM-17-OEt ($Cu(C_{10}O_5H_8)\bullet 1.6H_2O$), based on the 5-ethoxyisophthalate linker (STAM stands for St Andrews Material) using hydrothermal methods. The structure of STAM-17-OEt at 300 K and ambient pressure (Figure 1) was solved using single-crystal X-ray diffraction at the Advanced Light Source, Berkeley, USA.

The material crystallises in the trigonal space group $P\ \bar{3}m1$ with unit cell dimensions a = 18.576(12) Å and c = 6.8056(6) Å, and has the Kagome-type topology. The framework comprises four-connecting nodes, in this instance copper carboxylate paddlewheel units, bridged by the 5-ethoxy isophthalate linking units, to create an infinite two-dimensional framework (see Figure 1). Coordinated water molecules occupy the apical coordination site on each of the copper centres and form hydrogen bonds (O···O 3.072(3) Å) to the coordinated carboxylate oxygen atoms on the sheets above and below. All copper centres are crystallographically equivalent, as are all 5-ethoxy isophthalate anions. The ethyl group is disordered over two symmetry-related sites. The structure of this material is related to that of other copper-based MOFs that contain the Cu paddlewheels and are connected into porous structures by polycarboxylate bridging ligands. Examples of such MOFs

include HKUST-1,[12] STAM-1[19] and Cu(aip)[20] amongst many others. The Kagome lattice has two types of unidimensional channel extending through the sheet with either hexagonal or triangular cross sections. Coordinated water molecules project into the triangular channels, which also contain disordered guest water molecules. The hexagonal channels contain the disordered ethyl groups. As the sheets are eclipsed, both types of channel extend perpendicular to the Kagome sheets through the whole depth of the crystal.

Crystallographic studies after evacuation of the same single crystal of STAM-17-OEt using a sealed gas cell showed that the crystal had undergone a single-crystal-to-single-crystal transition, in which the unit cell of the crystal changes to a = 33.028(3) Å and c = 5.2047(6) Å. The dehydrated phase exists in space group $P31m$. All water molecules, both free and coordinated, have been removed and the framework is now composed of four crystallographically unique copper centres (arranged into two distinct copper paddlewheels) and four unique isophthalate ligands. In this dehydrated phase there are two crystallographically distinct hexagonal channels (one that contains disordered ethyl groups and one containing ordered ethyl groups) and two distinct triangular channels. The Kagome sheets have deformed such that on half of the copper paddlewheels, the coordination sites that were previously occupied by coordinated water molecules (Cu-O distance = 2.150(2) Å) are now occupied by μ_2-coordinated carboxylate oxygen atoms (Cu-O 2.24(2) Å or 2.19(3) Å) that belong to a paddlewheel unit in the sheet above or below. This change in coordination environment of the copper centres alters the dimensionality of the framework from two- to three-dimensional. The remaining half of the paddlewheels are arranged such that the copper centres of one lie almost equidistant between the carboxylate oxygen atoms on neighbouring paddlewheels with much longer Cu-O distances of 2.87(3) Å and 2.98(4) Å. This change in the coordination sphere of the copper centres (i.e. the hemilability) allows the weaker μ_2-O-CO groups to bind at sites that were vacated by the water molecules, rather than leaving these sites vacant. Powder X-ray diffraction (see supplementary information Fig. 4) and solid-state NMR experiments (see below) indicate that this transition occurs in the dehydration of bulk powders.

On exposure to moisture the crystal of STAM-17-OEt reverts to the original as-synthesised structure. To accomplish the change, energy must be used to break the weak interactions and move the paddlewheels relative to each other. The energy released on interaction of the adsorbed water with the framework metals is used to change the coordination and relative positions of the paddlewheel units and is not, therefore, available for breaking further bonds in the material.

NMR The change in structure of STAM-17-OEt on dehydration is easily seen in the ^{13}C solid-state NMR spectra shown in Figure 3. The paramagnetic nature of the copper ions in the material leads to a much wider shift range than typically observed for diamagnetic materials but for the analogous copper paddlewheel MOFs HKUST-1 and STAM-1 the shift range is well characterised and the resonances fully assigned.[21] By analogy, and using a combination of magic angle spinning (MAS) and cross-polarisation MAS experiments (See supplementary information Fig. 21), the resonances for STAM-17-OEt can be assigned as shown in Figure 3b. Note that the resonance for C1 (observed at ~830 ppm) is not shown in Figure 3 but is shown in supplementary information Fig. 20. The resonances for C3 and C5 are overlapped at 298 K but can be separated at higher temperature (Figure 3c).

In the hydrated material, the signals from each of the carbon atoms of the linker are present as single resonances (including those for the disordered carbons of the ethyl group, C6 and C7, suggesting rapid exchange between the possible orientations rather than static disorder). However, on dehydration there are significant changes to the local structure of STAM-17-OEt, and these are reflected in the ^{13}C NMR spectrum shown in Figure 3d. The single signal from this carbon atom in the hydrated material splits into four resolvable resonances for the dehydrated solid. These four resonances have an approximate intensity ratio of 1 : 1 : 1 : 3, which is entirely consistent with the six expected independent C2 carbons from the single-crystal X-ray diffraction structure (Figure 2). These changes in local structure are most pronounced for the carboxylate carbon, C2, as it is the closest to the paddlewheel units. As one moves further away from the paddlewheel units the

resonances are less and less affected by the structural changes. For example, the resonances for carbons C6 and C7 in the ethyl group, are not visibly affected at all by the structural changes.

Density functional theory (DFT) calculations were performed in order to quantify the energetics of the formation of the weak interactions in dehydrated STAM-17-OEt. To do this, two idealised model structures were generated from experimentally determined structures of dehydrated and hydrated STAM-17-OEt respectively, to give a model for the observed dehydrated material as shown in Figure 2. Removal of the water molecules from the rehydrated model produced a hypothetical dehydrated model where no movement of the paddlewheel units has been allowed, and therefore none of the weaker interactions occur. Both models were simplified by replacement of disordered ethoxy groups in the 5-position of the isophthalate linkers with hydrogen (i.e. giving STAM-17-H), and to allow direct comparison between the frameworks. The unit cell of the model derived by dehydration of the as-made material was transformed to make the unit cell contents equivalent in both cases. The structures were then optimised using the CASTEP package[22] under periodic, dispersion-corrected DFT, with all atomic positions and unit cell parameters allowed to vary (see Methods). Only subtle changes in the framework atomic positions were observed, resulting in near-superimposable computed and experimental structures. The difference in the calculated energies of the two models should be, to a first approximation, a measure of the energy needed to break the weaker copper-oxygen interactions and move the paddlewheels relative to each other. The observed dehydrated model was found to be 0.228 eV (i.e. 2.4 kJ mol^{-1} per Cu dimer) lower in energy than the hypothetical dehydrated model, supporting the proposal that the formation of the weak interactions adds thermodynamic stability to the system, which will require energy to overcome when rehydrating the material – energy that cannot then be used to break the structure down. Of course, this fairly simple analysis does not take into account the energy barriers to the structural changes on rehydration, which will increase the energy required for the transformation, further limiting the energy available to indiscriminately break bonds.

The practical significance of this effect is clear when one studies the adsorption of toxic gases for personal protection. MOFs are of great interest for the adsorption of toxic gases primarily because of their high capacity, but to be used in practical personal protection applications they must be robust in the presence of moisture, which is always present in breathable air. For many gases (e.g. those containing fairly soft elements such as nitrogen), copper-based MOFs would be an excellent choice, as there should be strong, selective interactions between the adsorbed gases and the framework.

Water stability The main question to be answered is whether STAM-17-OEt actually shows improved stability to water. Figure 4a shows the evolution of the mass of dehydrated HKUST-1 and STAM-17-OEt structures on exposure to a moist environment at 298 K. STAM-17-OEt shows an initial rapid increase in mass as the dehydrated material adsorbs water. There is then no further change over the remainder of the experiment (up to 5 days). HKUST-1 on the other hand shows a similar immediate mass gain as the water interacts with the open metal sites, but within the first hours the material begins to gain further mass as water molecules start to react with other copper sites that have been made available through degradation (Figure 5). This process continues until a maximum mass is reached at just under 20 hours. The molecular mechanism of this process has recently been elucidated and involves the successive breaking of metal to carboxylate oxygen bonds.[23,24] To accommodate increased water uptake during this period the water must be interacting with 'extra' copper sites that were not available in the initial dehydrated material. These are produced as water interacts with the open metal sites, releasing energy, which is used to break metal-carboxylate oxygen bonds in the structure. This opens up metal sites for further coordination to water,[23,24] which leads to the extra mass gain. As more of the bonds are successively broken there comes a time when there are not enough such bonds to hold the MOF intact, and so HKUST-1 begins to collapse releasing water during the process. Under the conditions of our experiment this leads to the loss of mass between 20 and 40 hours, after which time the mass stabilises as the entire HKUST-1 structure has been lost. In

contrast to HKUST-1, after the initial adsorption of water, with its associated mass gain, the mass of STAM-17-OEt remains unchanged throughout the remainder of the experiment. As demonstrated by the IR spectra, HKUST-1 undergoes significant change upon exposure to a humid atmosphere (Figure 4b), while the spectrum of STAM-17-OEt (Figure 4c) remains unchanged.

Cycling of the relative humidity between 0 and 90% at 298 K (8 hours for each cycle for a total of 120 hours) further illustrates the significant improvement in stability of STAM-17-OEt compared to HKUST-1. The maximum water uptake capacity of HKUST-1 decrease with every cycle while that of STAM-17-OEt samples remains constant throughout the experiment (Supplementary Figs 13 and 14). The PXRD of the recovered samples from the experiments show that once again HKUST-1 has lost its structure while STAM-17-OEt retains its crystallinity and structure (Supplementary Figures 5 and 6).

A longer-term experiment where STAM-17-OEt is left in contact with water for one year at room temperature showed no degradation in crystallinity of its structure (Supplementary Fig. 7). Given that HKUST-1 loses crystallinity in less than two days or so under comparable conditions it is clear that STAM-17-OEt has significantly enhanced hydrolytic stability compared to HKUST-1.

Toxic gas adsorption A very similar situation is seen in ammonia breakthrough experiments (see Methods) on samples that have been exposed to moisture for certain periods of time. On dehydrated samples that have only been treated with moisture, the ammonia adsorption capacity of HKUST-1 increases before eventually falling back to levels at or below the original capacity of HKUST-1 (Figure 4d). This cooperative ammonia/water adsorption has been noticed previously.[25] The ammonia capacity of STAM-17-OEt also increases slightly over the course of the experiments but we have not reached a plateau even after five days' exposure to 90% humidity indicating improved performance. Infrared spectroscopy (Figure 4e and 4f) again shows no difference between as-synthesised STAM-17-OEt and material that has been in contact with 90% humidity for 5 days.

The key question is why does the mechanism degrade the paddlewheel units in HKUST-1 but not the same units in STAM-17-OEt? Our proposed reasoning is shown in Figure 5. The 'crumple zone' mechanism described above for water adsorption on STAM-17-OEt effectively directs the energy produced away from the critical bonding that makes up the paddlewheel unit (Figure 5a), exactly like a crumple zone in an automobile directs energy from a collision away from the passengers in a road traffic accident. There is no such mechanism available in HKUST-1, and any energy released on adsorption of water on the open metal sites can be used to break a metal-oxygen bond in the paddlewheel, which then potentially opens up new metal sites for water adsorption. Initially this can lead to an apparent increase in adsorption capacity, as seen in Figures 4a and 4d. However, as this mechanism continues the structural integrity of the paddlewheel is compromised and the structure will fall apart.

There are other possible mechanisms that can affect the hydrolytic stability of the MOFs. There is a correlation between porosity and thermodynamic stability of porous solids that have been prepared using traditional solvothermal crystallisations. This is most well-known for zeolites[26] but also appears to be true for MOFs.[27,28] This can be seen in the DFT calculations described above, where the observed dehydrated model of STAM-17-OEt is 2.4 kJ mol^{-1} Cu lower in energy than the model derived from the hypothetical dehydrated structure, which would have higher porosity. However, this is a very small change in energy and is very unlikely to contribute strongly to the observed improvement in hydrolytic stability, although it is likely to be a very minor factor.

There is also the possibility that the comparisons we are making are not exactly like-for-like in terms of the chemistry. While the chemical composition of STAM-17-OEt is *close* to that of HKUST-1, it is not exactly the same. Could the change in electronic structure of the linker ligands be the most important factor in determining the differences in hydrolytic stability? Fortunately, the organic chemistry of the system means we can directly test this issue by varying the 5-substituent on the isophthalate linker. By changing this group from electron donating such as ethoxy (as

in STAM-17-OEt) to electron withdrawing such as methylcarboxy (-CO_2Me), which we call STAM-1- CO_2Me[19] we can vary the electronic properties of the ligand across a relatively wide range. STAM-1- CO_2Me behaves in exactly the same way as STAM-17-OEt: exposure to water for long periods, and repeated cycling of relative humidity between 0 and 90% at 298 K (8 hours for each cycle for a total of 120 hours) have no effect on the structure of the material (See supplementary information Figs 10 and 15). This proves that while there will certainly be an effect of changing the electronic properties of the linker, it cannot be the major reason for the improved stability.

Therefore, we are confident that the new crumple zone mechanism displayed by STAM-17-OEt is the major reason for the improved stability, and that it offers new possibilities to reduce the long-standing issues regarding the stability of activated MOFs (especially when challenged with nucleophiles such as water) by understanding and then carefully controlling features such as flexibility arising from hemilability. Such an approach may reduce problems of stability to levels that allow applications in many other areas than are now possible.

Methods

Synthesis of STAM-17-OEt. STAM-17-OEt was synthesised by heating $Cu(OAc)_2.H_2O$ (0.20 g, 1.00 mmol), 5-ethoxyisophthalic acid (0.21 g, 1.00 mmol) and distilled water (15 mL) in a stainless-steel autoclave at 383 K for 3 days. The autoclave contents were filtered upon cooling and the solid was washed with distilled water and ethanol, before drying in air. Yield was 0.24 g, 0.76 mmol, 76%.

Single crystal X-ray diffraction experiments

A single crystal of STAM-17-OEt was mounted on a MiTeGen® MicroGripper without protective oil and sealed inside an in-house built gas cell. Data were collected on a Bruker D8 diffractometer equipped with a PHOTON100 detector, on station 11.3.1 of the Advanced Light Source (λ = 0.7749(1) Å). An initial dataset was collected at 300(2) K at ambient pressure, before evacuating the cell for 15 minutes to 17 mTorr and collecting a second dataset under dynamic vacuum (down to 7 mTorr). Multi-scan absorption corrections were applied to both datasets using SADABS[29]. Structural solutions were obtained from SHELXT and refined on F^2 using SHELX-2014 within the ShelXle software.[30] Appropriate scattering factors were applied using the XDISP program[31] within the WinGX suite of programs.[32] For the hydrated phase, all full occupancy non-hydrogen atoms were refined with anisotropic thermal displacement parameters. Aliphatic and aromatic hydrogen atoms were included at their geometrically estimated positions, the hydrogen atom of the coordinated water molecule was located in the difference map and fixed at a distance of 0.90(2) Å from the oxygen atom to which it is bound. The ethyl group was found to be disordered over two symmetry-related sites, and the carbon atoms have been refined anisotropically with site occupancies of 50%. Residual peaks of electron density were assigned as the oxygen atoms of partial occupancy water molecules and given a fixed isotropic thermal displacement parameter of 0.08 while their occupancies were allowed to refine. For the dehydrated phase, the crystal had undergone significant structural rearrangement, which was reflected in the quality of the diffraction pattern. All aliphatic and aromatic hydrogen atoms were included at their geometrically estimated positions. The carbon-carbon bonds within the aromatic rings were restrained to have the same value, which was refined as a free variable, as the unrestrained C-C bond lengths within the rings ranged from 1.30 Å to 1.52 Å. The C-C bond lengths in the ethyl chains were also refined as a common free variable, whilst all C-CO_2 bonds were constrained to have equal lengths. Only Cu1 and Cu2 were refined with anisotropic thermal displacement parameters, the majority of the remaining atoms tended to turn non-positive definite when refined anisotropically, due to a combination of poor data quality and the potential disorder described below. Large positive and negative peaks of electron density surrounding the Cu3-Cu4 paddlewheel suggest that this unit exists in two positions within the

crystal, likely due to incomplete conversion of the crystal between the hydrated and dehydrated phases. Attempts were made to model this disorder, and a second orientation of Cu3, Cu4 and a large portion of the 5-ethoxy isophthalate ligand containing the C16 to C21 aromatic ring were modelled with an occupancy complementary to that of the major component. The ratio of these two components refined to 93:7. Given the less than ideal data quality of this second dataset, such a minor component would not provide any reliable structural data and these attempts were abandoned.

Powder X-ray diffraction Experiments were completed at room temperature using Cu Kα radiation or using synchrotron X-rays (λ = 0.8260 Å) using beamline I11 at the Diamond Synchrotron Light Source. Dehydrated samples were sealed inside capillaries to prevent exposure to atmospheric moisture. All experiments were carried out at 298 K.

MAS NMR The solid-state spectra were recorded using a Bruker Avance III spectrometer equipped with a wide-bore 9.4 T superconducting magnet (^{13}C Larmor frequency of 100.6 MHz). Samples were packed into 1.9 mm ZrO_2 rotors and rotated at the magic angle at rates of 37.5-40 kHz. Signal averaging was carried out for 14336-66560 transients with a repeat interval of 100 ms. A rotor-synchronised spin-echo pulse sequence (echo duration of one rotor period) was used to minimise the probe background signal. The temperature was calibrated using the position of the ^{87}Rb resonance of RbCl[33] and maintained using a Bruker BCU-II chiller and BVT/BVTB-3000 temperature controller. Shifts are reported in ppm relative to TMS using the CH_3 resonance of L-alanine (δ = 20.5 ppm) as a secondary solid reference.

Computational Details Geometry optimizations were performed using the CASTEP package[21] (version 16.11). Periodic density functional theory (DFT) calculations adopted the PBE exchange-correlation functional along with the Tkatchenko-Scheffler dispersion correction scheme. Default on-the-fly ultrasoft pseudopotentials were used with an energy cut-off of 50 Ry and included scalar relativistic effects through ZORA. Brillouin space was sampled using a Monkhorst-Pack grid with a k-point spacing of 0.04 2π Å^{-1}.

Water stability and ammonia adsorption Water stability was monitored using a Dynamic Vapour Sorption (DVS) (Surface Measurement Systems) apparatus, where a sample of material (approximately 20 mg) was placed in a stainless-steel pan. The relative humidity (RH) within the instrument was increased to 90% and sustained over the course of 5 days (298 K), and the mass of the sample monitored.

Humidity cycling experiments were also completed in a DVS system by changing the relative humidity from 0 to 90% every eight hours. The temperature was held constant at 298 K and the mass of the samples monitored. The experiments lasted 120 hours (eight full cycles).

Ammonia micro-breakthrough testing was performed using a micro breakthrough apparatus. The setup allows testing of MOF materials against known concentrations of gases under either dry or humid (RH = 80%) conditions. Samples of approximately 20 mg were packed between two cotton wool plugs in a glass tube with an internal diameter of 4mm. Ammonia gas with a concentration of 500 ppm was passed through the sample at a flow rate of 30 mL/min and the challenge gas output concentration was monitored using a handheld VOC gas detector ("Phocheck Tiger" PID detector). All experiments were completed at 298 K.

Data availability All data generated and analysed during this study are included in this Article and its Supplementary Information, and are also available from the authors upon reasonable request. Atomic coordinates and structure factors for the reported crystal structures have been deposited in the Cambridge Crystallographic Data Centre (www.ccdc.cam.ac.uk) under accession codes 1566114 and 1566115. The data can also be accessed at http://dx.doi.org/10.17630/947f0bbe-b5b3-447d-bc59-07252966f1ed.

References

1. Zhou, H.C., Long, J.R. & Yaghi, O.M. Introduction to Metal-Organic Frameworks. *Chem. Rev.* **112**, 673-674 (2012)
2. Sumida, K.*, et al.* Carbon Dioxide Capture in Metal-Organic Frameworks. *Chem. Rev.* **112**, 724-781 (2012)
3. Suh, M.P., Park, H.J., Prasad, T.K. & Lim, D.W. Hydrogen Storage in Metal-Organic Frameworks. *Chem. Rev.* **112**, 782-835 (2012)
4. McKinlay, A.C.*, et al.* BioMOFs: Metal-Organic Frameworks for Biological and Medical Applications. *Angew. Chem.* **49**, 6260-6266 (2010)
5. Ferey, G. & Serre, C. Large breathing effects in three-dimensional porous hybrid matter: facts, analyses, rules and consequences. *Chem. Soc. Rev.* **38**, 1380-1399 (2009)
6. Burtch, N.C., Jasuja, H. & Walton, K.S. Water Stability and Adsorption in Metal-Organic Frameworks. *Chem. Rev.* **114**, 10575-10612 (2014)

7. Cavka, J.H.*, et al.* A new zirconium inorganic building brick forming metal organic frameworks with exceptional stability. *J. Am. Chem. Soc.* **130**, 13850-13851 (2008).
8. Colombo, V.*, et al.* High thermal and chemical stability in pyrazolate-bridged metal-organic frameworks with exposed metal sites. *Chem. Sci.* **2**, 1311-1319 (2011)
9. DeCoste, J.B., Denny, M.S., Peterson, G.W., Mahle, J.J. & Cohen, S.M. Enhanced aging properties of HKUST-1 in hydrophobic mixed-matrix membranes for ammonia adsorption. *Chem. Sci.* **7**, 2711-2716 (2016)
10. DeCoste, J.B., Peterson, G.W., Smith, M.W., Stone, C.A., Willis, C.R. Enhanced Stability of Cu-BTC MOF via Perfluorohexane Plasma-Enhanced Chemical Vapor Deposition. *J. Am. Chem. Soc.* **134**, 1486-1489 (2012).
11. Wittmann, T.*, et al.* Enhancing the Water Stability of Al-MIL-101-NH2 via Postsynthetic Modification. *Chem-Eur J* **21**, 314-323 (2015).
12. Chui, S.S.Y., Lo, S.M.F., Charmant, J.P.H., Orpen, A.G. & Williams, I.D. A chemically functionalizable nanoporous material Cu-3(TMA)(2)(H2O)(3) (n). *Science* **283**, 1148-1150 (1999).
13. Peterson, G.W.*, et al.* Ammonia Vapor Removal by Cu-3(BTC)(2) and Its Characterization by MAS NMR. *J. Phys. Chem C* **113**, 13906-13917 (2009)
14. DeCoste, J.B. & Peterson, G.W. Metal-Organic Frameworks for Air Purification of Toxic Chemicals. *Chem. Rev.* **114**, 5695-5727 (2014)
15. Singh, M.P., Dhumal, N.R., Kim, H.J., Kiefer, J. & Anderson, J.A. Influence of Water on the Chemistry and Structure of the Metal Organic Framework Cu-3(btc)(2). *J. Phys. Chem C* **120**, 17323-17333 (2016).
16. Serre, C.*, et al.* Very large breathing effect in the first nanoporous chromium(III)-based solids: MIL-53 or Cr-III(OH)center dot{O2C-C6H4-CO2}center dot{HO2C-C6H4-CO2H}(x)center dot H2Oy. *J. Am. Chem. Soc* **124**, 13519-13526 (2002)
17. Xiao, B.*, et al.* Chemically blockable transformation and ultraselective low-pressure gas adsorption in a non-porous metal organic framework. *Nat. Chem.* **1**, 289-294 (2009).

18. Slone, C.S., Weinberger, D.A. & Mirkin, C.A. The transition metal coordination chemistry of hemilabile ligands. *Prog. Inorg. Chem. Vol 48* **48**, 233-350 (1999).
19. Mohideen, M.I.H.*, et al.* Protecting group and switchable pore-discriminating adsorption properties of a hydrophilic-hydrophobic metal-organic framework. *Nat. Chem.* **3**, 304-310 (2011)
20. Sato, H.*, et al.* Self-Accelerating CO Sorption in a Soft Nanoporous Crystal. *Science* **343**, 167-170 (2014)
21. Dawson, D.M.*, et al.* High-resolution solid-state C-13 NMR spectroscopy of the paramagnetic metal-organic frameworks, STAM-1 and HKUST-1. *Phys. Chem. Chem. Phys.* **15**, 919-929 (2013)
22. Clarke, S.J. *et al.* First principles methods using CASTEP *Z. Kristall.* **220**, 567-570 (2005).
23. Al-Janabi, N., Alfutimie, A., Siperstein, F.R. & Fan, X.L. Underlying mechanism of the hydrothermal instability of Cu-3(BTC)(2) metal-organic framework. *Frontiers Chem. Sci. Eng.* **10**, 103-107 (2016)
24. Todaro, M.*, et al.* Decomposition Process of Carboxylate MOF HKUST-1 Unveiled at the Atomic Scale Level. *J. Phys. Chem. C* **120**, 12879-12889 (2016)
25. Nijem, N., Fursich, K., Bluhrn, H., Leone, S.R. & Gilles, M.K. Ammonia Adsorption and Co-adsorption with Water in HKUST-1: Spectroscopic Evidence for Cooperative Interactions. *J. Phys. Chem. C* **119**, 24781-24788 (2015)
26. Mazur, M.*, et al.* Synthesis of 'unfeasible' zeolites. *Nat. Chem.* **8**, 58-62 (2016)
27. Morris, R.E. & Cejka, J. Exploiting chemically selective weakness in solids as a route to new porous materials. *Nat. Chem.* **7**, 381-388 (2015)
28. Wu, D. & Navrotsky, A. Thermodynamics of metal-organic frameworks. *J. Solid State Chem.* **223**, 53-58 (2015)
29. Krause, L., Herbst-Irmer, R., Sheldrick, G. M. & Stalke, D. Comparison of silver and molybdenum microfocus X-ray sources for single-crystal structure determination *J. Appl. Crystallogr.* **48**, 3-10 (2015)
30. Sheldrick, G. M. Crystal structure refinement with *SHELXL Acta. Cryst C.* **71**, 308 (2015)

31. Brennan, S. & Cowan, P.L. A suite of programs for calculating x-ray absorption, reflection, and diffraction performance for a variety of materials at arbitrary wavelengths *Rev. Sci. Instrum.* **63**, 850-853 (1992)
32. Farrugia, L.J. WinGX and ORTEP for Windows: an update *J. Appl. Cryst.* **45**, 849-854 (2012)
33. Skibsted, J. & Jakobsen, H. J. Variable-Temperature ^{87}Rb Magic-Angle Spinning NMR Spectroscopy of Inorganic Rubidium Salts *J. Phys. Chem. A*, **103**, 7958-7971 (1999)

Acknowledgements R.E.M. thanks the Royal Society and the EPSRC (Grants EP/L014475/1, EP/K025112/1) for funding work in this area and the Czech Science Foundation for the project P106/12/G015 and OP VVV "Excellent Research Teams", project No. CZ.02.1.01/0.0/0.0/15_003/0000417 – CUCAM. SEA thanks the Royal Society/Wolfson Foundation for a merit award, and the European Research Council (EU FP7 Consolidator Grant 614290 "EXONMR") for funding. This research used resources of the Advanced Light Source, which is a US DOE Office of Science User Facility under contract no. DE-AC02-05CH11231 and the development of the gas cell used in this research was funded through US DOE award # DE-SC0001015. We also thank Diamond Light Source and Chiu Tang for access to beamline I11. We thank Mr Simon Vornholt for help with the electron microscopy and the EPSRC Capital for Great Technologies funding (EP/L017008/1).

Additional information

Reprints and permissions information is available online at www.nature.com/reprints. Correspondence and requests for information should be addressed to R.E.M. (rem1@st-and.ac.uk).

Author Contributions

L.J.M. originally synthesised the material and completed the crystallography with S.A.M. and S.J.T. The adsorption and stability experiments were designed and carried out by L.N.M., P.S.W., M.J.M., C.A.S. and M.W.S. The NMR was completed and

analysed by D.M.D., C.E.F.S. and S.E.A, and D.M. carried out the computational work. The paper was written by L.N.M. and R.E.M. and revised by all authors.

Competing financial interests

The authors declare no competing financial interests.

Figures

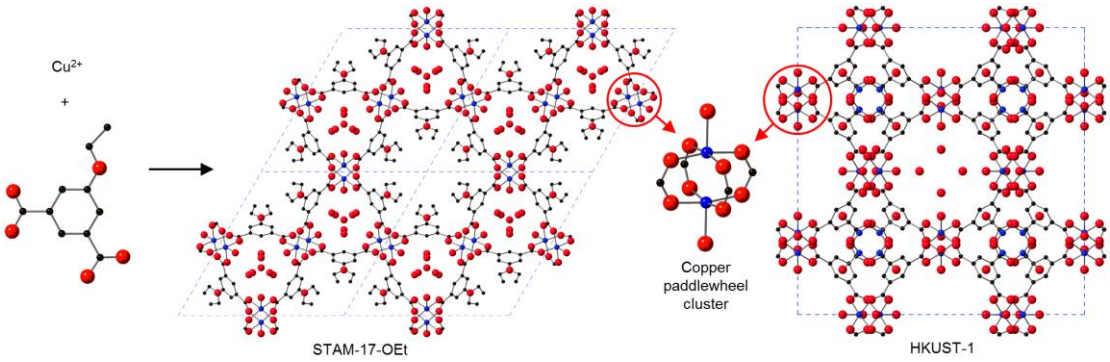

Figure 1. The structure of STAM-17-OEt showing the paddlewheel dimer present in the structure. Note that the ethyl groups are disordered over two possible sites, each 50% occupied. The structure of HKUST-1, highlighting the presence of the same paddlewheel dimer, is shown for comparison. Colour key: Blue spheres = Cu, red = O, black = C. Hydrogen atoms have been omitted for clarity.

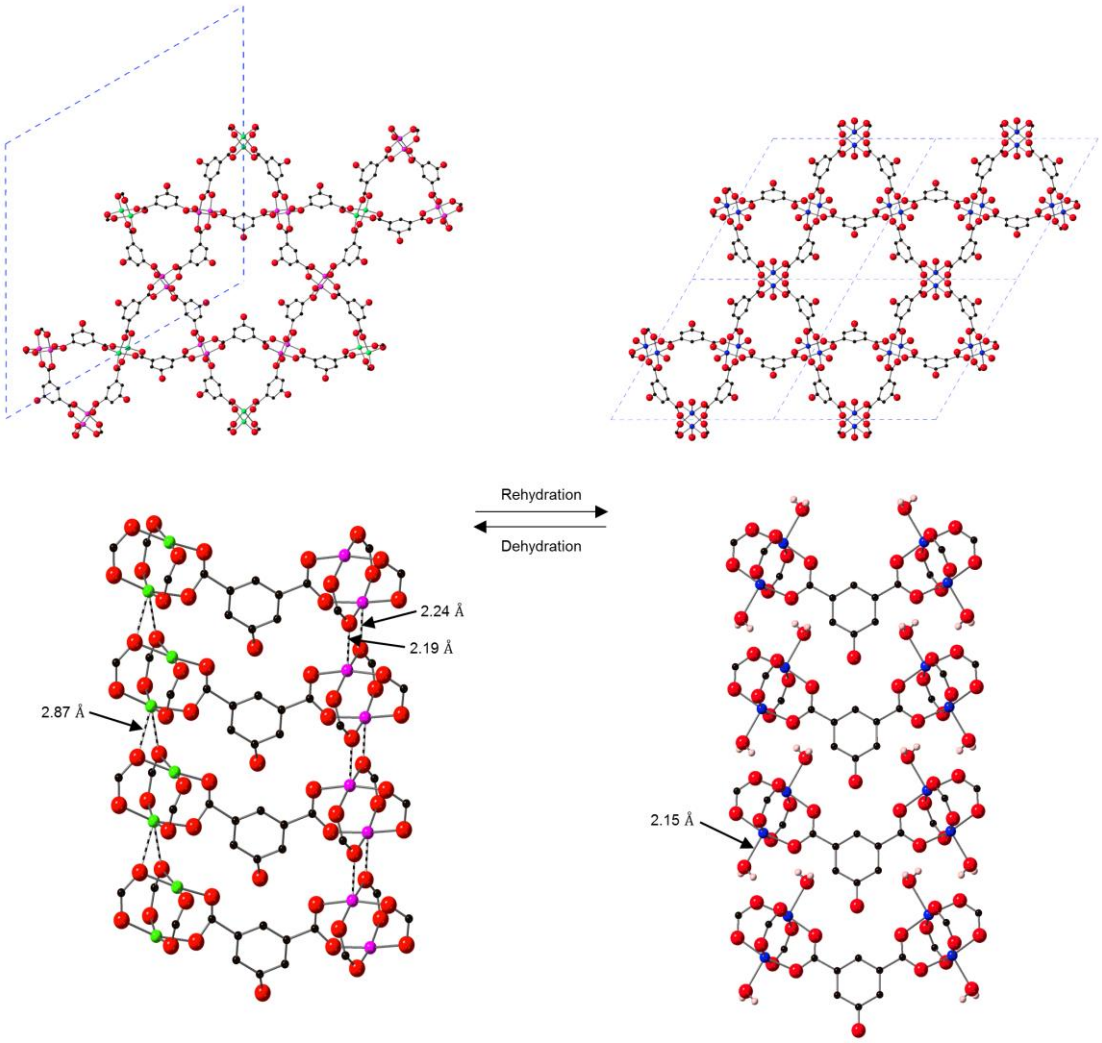

Figure 2. **The structural change on rehydration of dehydrated STAM-17-OEt**. The longer Cu···O interactions (indicated by the dotted bonds) are broken and replaced by stronger Cu-OH_2 interactions. Colour key: Blue, green or pink spheres = Cu (in different local environments), red = O, black = C. Aromatic and alkyl hydrogen atoms, and the carbon atoms of the alkyl chains, have been omitted for clarity.

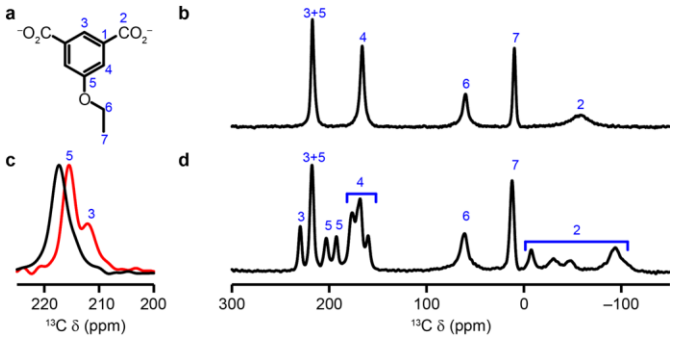

Figure 3. Solid-state ^{13}C NMR data for as-made and dehydrated STAM-17-OEt. (a) Numbering scheme for the chemically distinct C atoms in STAM-17-OEt. (b) ^{13}C (14.1 T, 37.5 kHz MAS, 298 K) NMR spectrum of as-made STAM-17-OEt. (c) Expansion of the C3+C5 resonance of as-made STAM-17-OEt at 298 K (black) and 338 K (red), where the two signals are resolved at the higher temperature. (d) ^{13}C (14.1 T, 40 kHz MAS, 298 K) NMR spectrum of dehydrated STAM-17-OEt.

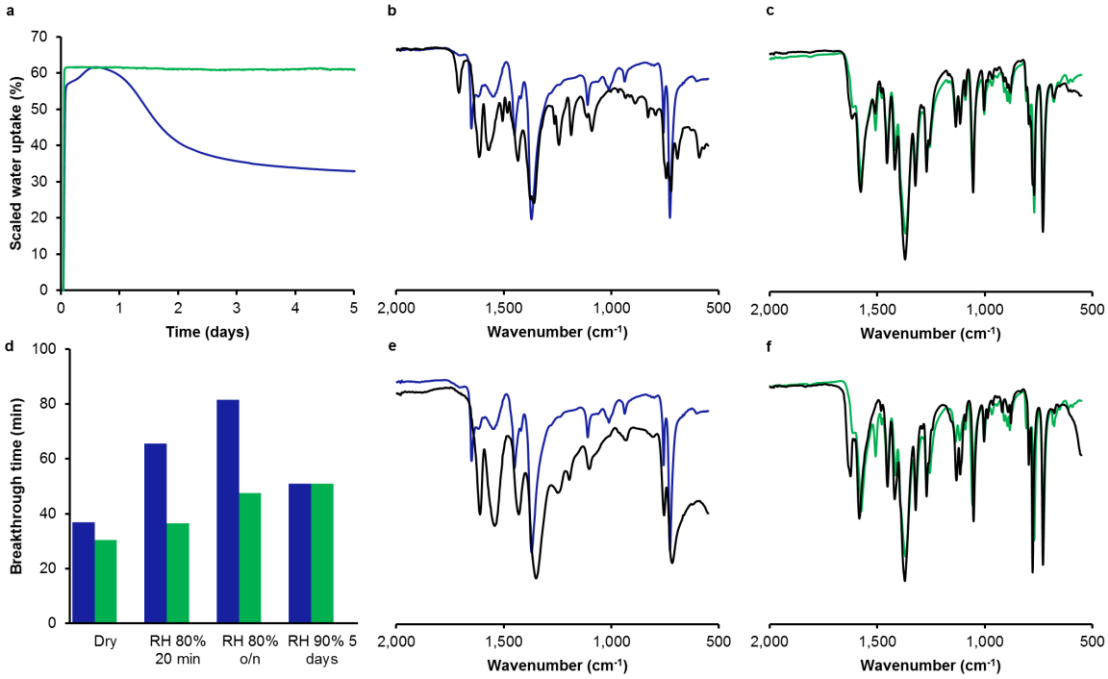

Figure 4. The water stability and ammonia adsorption capacities of STAM-17-OEt and HKUST-1. (a) Overlaid traces of the evolution of total mass of samples of dry STAM-17-OEt (green line) and dry HKUST-1 (blue line) on exposure to an atmosphere of 90% humidity over a period of 5 days. (b) and (c) The IR spectra for HKUST-1 and STAM-17-OEt, respectively. In each panel, the coloured trace shows the original material and the black trace after exposure to 90% humidity for 5 days. The spectra show that the spectrum for HKUST-1 changes significantly on exposure to water while that of STAM-17-OEt is unchanged. (d) The breakthrough time to reach 10% of influent concentration for ammonia on HKUST-1 (blue) and STAM-17-OEt (green). (e) and (f) The IR spectra for HKUST-1 and STAM-17-OEt, respectively, after exposure to ammonia. In each panel, the coloured trace shows the original material and the black trace after exposure to 90% humidity for 5 days. All experiments were conducted at 298 K.

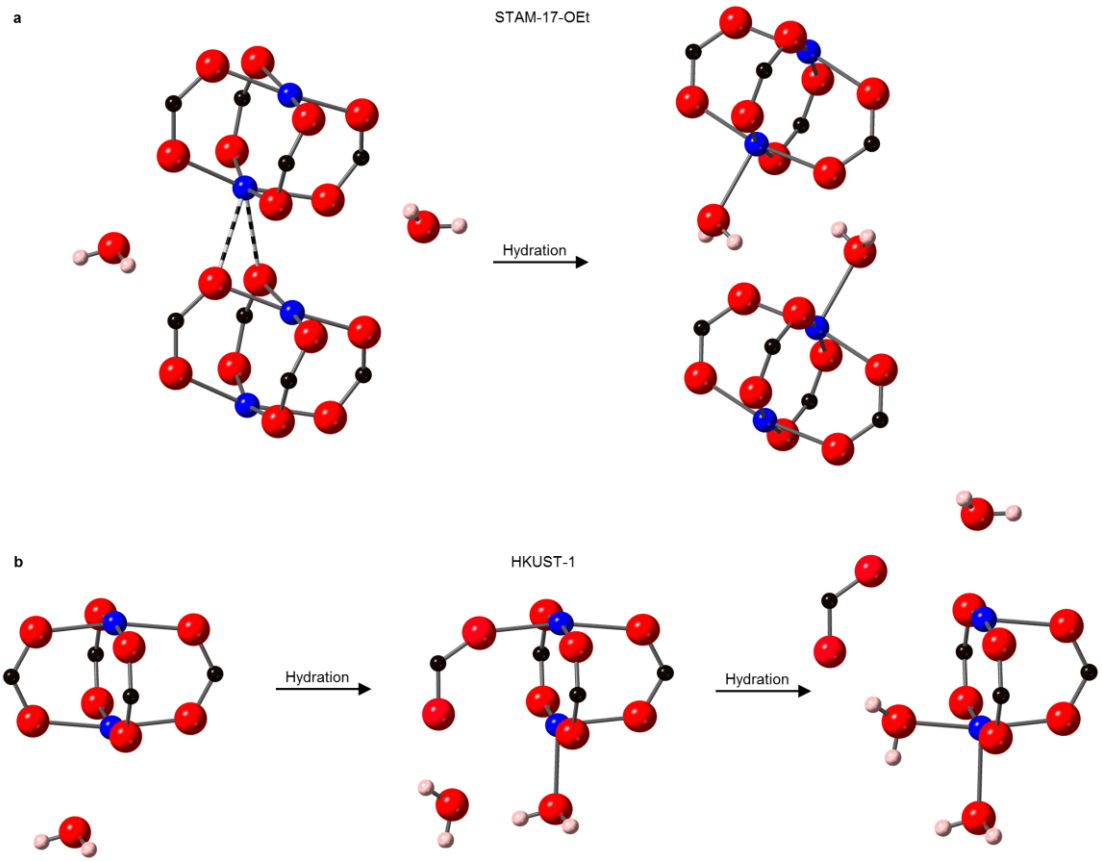

Figure 5 The effect of hydration on paddlewheel units in STAM-17-OEt and HKUST-1. (a) The mechanism of water adsorption on dehydrated STAM-17-OEt. The energy released by water adsorption onto the one open metal site in the structure releases energy that is then used to break the weak Cu···O interactions and move the paddlewheel units relative to each other. (b) The mechanism of paddlewheel breakdown in HKUST-1 (adapted from reference 24) where the adsorption of water onto the open metal sites in HKUST-1 can release energy that can then be used to break metal-carboxylate oxygen bonds in the paddlewheel, opening up further sites for more water adsorption, leading to the breaking of another metal-carboxylate oxygen bond and eventual breakdown of the HKUST-1 structure. Colour key: blue spheres = Cu; red = O; black = C and pink = H.